Carbohydrate Polymers 90 (2012) 709–716

Contents lists available at SciVerse ScienceDirect

Carbohydrate Polymers

journal homepage: www.elsevier.com/locate/carbpol

Biocomposites reinforced with cellulose nanocrystals derived from potato peel waste

D. Chen [a], D. Lawton [a], M.R. Thompson [a,*], Q. Liu [b]

[a] MMRI/CAPPA-D, Department of Chemical Engineering, McMaster University, Hamilton, Ontario, Canada L8S 4L7
[b] Guelph Food Research Centre, Agriculture and Agri-Food Canada, Guelph, Ontario, Canada

ARTICLE INFO

Article history:
Received 10 February 2012
Received in revised form 16 May 2012
Accepted 2 June 2012
Available online 9 June 2012

Keywords:
Cellulose nanocrystal
Polymer nanocomposite
Water vapor transmission
Tensile properties

ABSTRACT

This study investigated the effectiveness of cellulose nanocrystals derived from potato peel waste as a reinforcement and vapor barrier additive. The nanocrystals were derived from cellulosic material in the potato peel by alkali treatment and subsequently acid hydrolysis. TEM images revealed the average fiber length of the nanocrystals was 410 nm with an aspect ratio of 41; its aspect ratio being considerably larger than cotton-derived nanocrystals prepared using similar reaction conditions. Cellulose nanocrystals (CNC)-filled polyvinyl alcohol (PVA) and thermoplastic starch (TPS) films were prepared by solution casting method to maintain uniform dispersion of the 1–2% (w/w) filler content. An increase of 19% and 33% (starch composite) and 38% and 49% (PVA composite) in tensile modulus was observed for the 1% and 2% CNC-reinforced composites, respectively. Water vapor transmission measurements showed a marginal reduction of water permeability for the PVA composite, whereas no effect was observed for the thermoplastic starch composite.

1. Introduction

Cellulose is a sustainable, abundant biopolymer derived from a variety of living species such as plants, animals, bacteria and some amoebas. An attractive source of cellulose for industrial uses is agricultural waste, as this use does not jeopardize food supplies and improves the rural economy. Potato is a particularly important source of agricultural waste due to its significance as a crop for human consumption and the current demands within developed countries for its processing into fast food products (Keijbets, 2008). The large quantities of peel waste from processed potatoes have negligible value and most are discarded, with minor quantities sold at very low prices for supplementary animal feed (Tawali, Omer, & Gad, 2008). A second and no less significant source of waste from potatoes occurs as a result of heavy rainfalls which forces crops to be left in the ground to rot, causing substantial financial loss to farmers unless an alternative industrial use can be found for the biomass. The extracted cellulose from this source of waste biomass represents only a small fraction (~2%; Tawali et al., 2008) of the dry solids content of a potato and so its conversion should only be considered for high-value products to justify the processing expense.

Cellulose microfibrils extracted from potato pulp were previously demonstrated as an effective reinforcing additive (Dufresne, Dupeyre, & Vignon, 2000). The microfibrils exhibited diameters in the order of 10 nm and lengths of 10–100 μm, prepared by alkaline washing, bleaching and finally mechanical attrition. These long fibers retained amorphous regions which weakened their stiffness whereas cellulose nanocrystals remove this structural defect by subsequent processing steps (Hamad, 2008). The purpose of the present study was to remove these weaker domains from the cellulose by preparing nanocrystals from potato peel waste for the purpose of being a high value-adding reinforcing aid for polymer matrix composite manufacturing. This will be the first paper to prepare nanocrystals from potato peel waste in this regards for use as a functional filler in plastics.

Cellulose nanocrystals (CNC) are a promising material and have been widely studied over the past two decades. Broad ranges of uses have been speculated for this new nanomaterial by industry which include structural plastics, smart coatings, cosmetics, pharmaceuticals, solar energy collection, and with many more uses still being assessed (Eichhorn, 2011; Habibi, Lucia, & Rojas, 2010). These rod-like particles are commonly prepared by acid hydrolysis using strong acids (Azizi Samir, Alloin, & Dufresne, 2005). In the present work, our interest in this material is as a nanofiller, since it possesses nanoscale dimensions, high specific area, and highly rigid crystalline structure. In comparison to mineral or metal nanofillers that are industrially available, cellulose nanocrystals are prepared from renewable feedstocks, feature low density, are relatively low cost compared to many other synthetic nanofillers, and remain

Abbreviations: CNC, cellulose nanocrystal; ASTM, American standard test method; TPS, thermoplastic starch; XRD, X-ray diffraction; FTIR, Fourier transform infrared; WVTR, water vapor transmission rate.

* Corresponding author. Tel.: +1 905 525 9140x23213; fax: +1 905 521 1350.
E-mail address: mthomps@mcmaster.ca (M.R. Thompson).

0144-8617/$ – see front matter © 2012 Elsevier Ltd. All rights reserved.
http://dx.doi.org/10.1016/j.carbpol.2012.06.002

biodegradable (Azizi Samir et al., 2005; Dufresne, 2010). Due to these advantages, the field of CNC is intensifying with some of the considered applications being for mechanical reinforcement or improving the barrier properties of a polymer matrix.

The nanoscale dimensions of CNC along with their high inherent rigidity make them highly attractive for increasing the stiffness of polymer composites; the Young's modulus of a CNC is estimated to be 167.5 GPa which is comparable to that of Kevlar (Tashiro & Kobayashi, 1991). Cao, Dong, and Li (2007) reported a significant increase in Young's modulus and tensile strength once the incorporation of flax cellulose nanocrystals into waterborne polyurethane (WPU) exceeded a 10 wt% loading. Similarly, a 100% increase in Young's modulus was observed in a recent study using 5% cellulose nanocrystals from microcrystalline cellulose or flax cellulose to reinforce polyvinyl alcohol composites (Qua, Hornsby, Sharma, Lyons, & McCall, 2009). Improvements to the barrier property of a polyvinyl alcohol membrane by CNC addition were demonstrated by Paralikar, Simonsen, and Lombardi (2008) who experienced a significant reduction in water vapor and organic vapor (i.e. trichloroethylene) transmission for their prepared composite with 10% cotton CNC compared to a neat polymer. Pereda, Amica, Rácz, and Marcovich (2011) found that barrier properties to water vapor transmission improved when using up to 1% loading of CNC in caseinate films but then subsequently decreased with higher loadings due to increased defects in the matrix.

This paper compares the physical features and reinforcement properties of CNC derived from potato peel waste to similar CNC prepared from cotton cellulose which has been receiving considerable attention in the literature (Dong, Revol, & Gray, 1998; Lu & Hsieh, 2010; Paralikar et al., 2008). Purified yields of potato and cotton-derived CNC were incorporated into solution-cast polymer films prepared from starch and polyvinyl alcohol at concentrations of 0–2% (w/w) and then tested for mechanical and water absorption/transmission properties.

2. Materials and methods

2.1. Materials

Russet Burbank potatoes from Prince Edward Island, Canada were purchased from a local supermarket. A food-grade unmodified potato starch was provided by Manitoba Starch Products (Carberry, Manitoba, Canada). Polyvinyl alcohol (PVA, 87–89% partially hydrolyzed, M_w 50,000 Da) was purchased from Mallinckrodt Baker Inc. (Phillipsburg, NJ, USA). Sulfuric acid (95–98%), sodium chlorite (>80%) and sodium sulfate (Na_2SO_4, >99.0% purity) were supplied from Sigma–Aldrich (St. Louis, MO, USA), sodium hydroxide (pellet) was purchased from EMD Chemical (San Diego, CA, USA), and glycerol (99.7%) was obtained from Caledon Laboratories Ltd. (Georgetown, ON, Canada).

2.2. Methods

2.2.1. Extraction of cellulose

The potatoes were hand-peeled and the removed mass was washed with water to rinse away soil and other bulk contaminants attached on the skins. The cleaned peels were added into water at a water-to-pulp ratio of 20:1 and agitated as a slurry using a blender for 10 min to remove the majority of potato flesh. The resulting slurry was filtered using a 250 μm sieve and repeatedly washed with distilled water. Potato peel waste is comprised of starch, cellulose, hemicellulose, lignin and other impurities, and therefore required several pretreatment steps including alkali treatments and chlorite bleaching (Dinand, Chanzy, & Vignon, 1996) to isolate its cellulosic component prior to acid hydrolysis. Initially, the peel waste was treated with a 0.5 N aqueous sodium hydroxide solution at 80 °C for 2.5 h under mechanical agitation. The treatment was done three times in order to completely eliminate the lignin, hemicellulose, and other impurities. After each treatment, the pulp was filtered and washed with distilled water using a 75 μm sieve to remove the alkali solution and dissolved impurities. The alkali washing was followed by bleaching with 2.3 wt% sodium chlorite solution in an acetate buffer (pH = 4.9). The purpose of the bleaching was to remove any organic residues. The bleaching treatment was carried out twice at 70 °C for 2 h each time. The extracted cellulose fibers from the potato were washed, freeze-dried and weighed.

The source of cotton cellulose used in the experiments was obtained from the bleached cellulose fibers in Whatman No. 1 filter paper (Whatman Inc.; Piscataway, NJ, USA). Filter paper was cut into 10 mm × 10 mm pieces and ground into dry pulp using a blender.

2.2.2. Preparation of cellulose nanocrystals

The optimized hydrolysis conditions reported for cotton cellulose were used for this study (Dong et al., 1998). The cellulose mass (potato or cotton) was added to deionized water along with 64 wt% sulfuric acid to give a pulp-to-acid ratio of 1:17.5 g/ml. The hydrolysis of cellulose was carried out at 45 °C under agitation by a mechanical stirrer. A reaction time of 60 min was found suitable for cotton; however, a longer time of 90 min was necessary for potato cellulose in order to obtain well separated nanocrystals. At the end of the reaction, an equivalent volume of distilled water was added to the acidic solution and then the cellulosic matter was separated from the mother liquor by centrifuge. Centrifuging of the product was repeated with fresh water until a turbid supernatant was obtained. The nanocrystal suspension was then dialyzed using Spectra/Por® membrane tubing rated for MWCO = 12–14,000 Da (Spectrum Laboratories Inc.; Rancho Dominguez, CA, USA) by immersion in distilled water for about 10 days, with the water being changed frequently. Neutralization of the suspension was confirmed by measuring the pH of the dialysis water until it ceased to change (i.e. pH ~ 6.5) before the sample was collected. The collected aqueous suspensions of cellulose nanocrystals were stored in plastic tubes at 4 °C till ready for use. If the fibers fell out of solution during storage, the sample was discarded.

2.2.3. Characterization of the cellulose nanocrystals

2.2.3.1. CNC morphology. Dimensions and the state of aggregation for the extracted CNC were observed using a JOEL TEMScan transmission electron microscopy (TEM) (JOEL Inc., Tokyo, Japan) at an acceleration voltage of 80 kV. A drop of highly diluted (0.001%, w/v) CNC suspension was deposited on a 100 mesh copper grid and allowed to dry. To improve the phase contrast of the fibers in the image, a drop of 2 wt% uranyl acetate was placed onto the grid and allowed to stand for 1 min before the excess liquid was wicked off with filter paper. Particle lengths and diameters were measured directly from the micrographs and a length distribution was obtained from analysis of over 200 CNC particles for each sample using Image J 1.44 visualization software (National Institute of Health, USA).

2.2.3.2. Infrared analysis. Fourier transform infrared (FTIR) spectra were measured from 400 to 4000 cm^{-1} at a resolution of 2 cm^{-1} using a Nicolet 6700 spectrometer (Thermo Fisher Scientific; West Palm Beach, FL, USA). Freeze-dried CNC samples were ground into a fine powder using a mortar and pestle, mixed with KBr and pressed into thin pellets.

2.2.3.3. X-ray diffraction. The crystalline structures of CNC were characterized by X-ray diffraction (XRD) collected on a Bruker D8 Advance Power diffractometer with Cu Kα radiation (λ = 1.54 Å)

(Bruker AXS Inc.; Madison, WI, USA) for a 2θ range from 5° to 40° at a scanning rate of 5°/min. The crystallinity index (C_I) was calculated using the equation by Segal, Creely, Martin, and Conrad (1959),

$$C_I = \frac{I_{002} - I_{am}}{I_{002}} \quad (1)$$

where I_{am} is the baseline intensity taken at $2\theta = 18°$ between the (0 0 2) and (1 0 $\bar{1}$) peaks in the diffraction pattern as characteristic of the amorphous regions in the cellulose and I_{002} is the intensity the (0 0 2) diffraction peak at $2\theta = 22.6°$ which is associated with the crystalline region of cellulose (Ostenson, Jarund, Toriz, & Gatenholm, 2006).

2.2.4. Preparation of thermoplastic starch nanocomposite films

Thermoplastic starch (TPS) being a sustainable bioplastic with increasing industrial attention made it an interesting material to test as to whether CNC could improve its mechanical and water absorption/transmission barrier properties. Potato starch was gelatinized at 80 °C for 30 min in a 4 wt% aqueous solution, to which a sample CNC/water suspension was added. Glycerol was added at 30% (w/w, db: dry basis relative to the polymer matrix) to the gelatinized starch solution as a plasticizer. The mixture was degassed by sonication for 15 min followed by vacuum for 1 h. Three different starch-based films were prepared with 0%, 1% and 2% (w/w, db) CNC using a solution casting method. The water was allowed to evaporate from the polymer suspension under laminar air flow at room temperature for 3 days before the film was removed from its 100 mm petri dish and then stored in an environmentally controlled room at 50% RH and 23 °C for at least 2 days before testing.

2.2.5. Preparation of polyvinyl alcohol nanocomposite films

Polyvinyl alcohol is another biodegradable polymer like thermoplastic starch but whereas starch has comparable chemical structure to cellulose, this polymer matrix will exhibit less compatibility with the CNC being tested as a nanoscale reinforcing (and barrier) agent. A 10 wt% PVA solution was made up by mixing the polymer granules supplied with distilled water and a sample of CNC in water suspension. The PVA granules were first left in distilled water at room temperature while being mechanical stirred overnight. Subsequently, the mixture was transferred to a water bath heated to 70 °C and mechanical agitation continued for 2 h till the polymer had completely dissolved. To the solution, 30% (w/w, db) glycerol was added as a plasticizer for consistency with the composition of the thermoplastic starch films. The CNC suspension (0, 1, 2% (w/w, db)) was slowly added into the stirred PVA solution in a dropwise manner once the polymer fully dissolved. The mixing continued for another hour, followed by 15-min sonication. The cooled mixture was poured into 100 mm petri dishes and the water was allowed to evaporate under laminar air flow at room temperature for 2 days. The films were demolded and stored in an environmentally controlled room at 50% RH and 23 °C for at least 2 days before testing.

2.2.6. Characterization of the polymer–nanocrystalline cellulose composites

2.2.6.1. Thermal analysis. The crystal melting transitions of the neat and CNC-filled polymer films were analyzed using a Q200 differential scanning calorimeter (DSC) by TA Instruments (New Castle, DE, USA). 5–7 mg samples were tested in aluminum Tzero hermetic DSC pans over a temperature range of −10 °C to 230 °C at a heating rate of 10 °C/min. A nitrogen flow was maintained at 50 mL/min during DSC tests. The second heating cycle was used for determining the melting enthalpy (ΔH_m) and its corresponding peak melting temperature (T_m) in order to evaluate changes in material crystallinity arising from the addition of CNC into the polymer matrix.

2.2.6.2. Film morphology. The state of dispersion for the CNC fillers within the polymer matrix of our prepared films was examined by scanning electron microscope (SEM) on a JEOL JSM-7000F (JEOL Ltd., Japan) at 5 kV. The film samples were dried overnight under vacuum at 40 °C and then prepared by cryogenically fracturing to expose their cross-sections for examination. To improve contrast in the SEM, the specimens were sputter-coated with a 5 nm layer of platinum prior to analysis.

2.2.6.3. Mechanical testing. Tensile testing was carried out with a Model 4411 Universal mechanical testing system (UMTS) (Instron Corporation; Norwood, MA, USA) located in an environmentally controlled room (50% RH and 23 °C) according to ASTM D882. The films were cut into 5 mm × 80 mm rectangular strips. The thickness of each specimen was measured before testing, though being generally ~150 μm thick. Measurements were performed with a 30 mm grip separation, 500 N load cell and a crosshead speed of 500 mm/min for PVA films and 10 mm/min for starch films. A minimum of five specimens were tested for each sample.

2.2.6.4. Water vapor transmission testing. The diffusion rate of water vapor through the films was determined according to ASTM E96 with modification. The exposed film area used for the tests was smaller than the standard due to the limited space available in the controlled environment, but this change did not affect the analysis since the tests were done on a comparative basis. Each cylindrical glass jar was 8 mm tall and had a 3 cm diameter mouth opening, which was filled with distilled water to a level of 19 ± 6 mm. Each film sample (thickness of ~150 μm) was placed over the mouth opening of a jar and sealed with a flanged clamp. The test assemblies were weighed and placed on a horizontal surface in a controlled environment at 50% RH and 23 °C. The test assemblies were weighed frequently, recording the weight change. The rate of water vapor transmission (WVT) can be calculated as:

$$\mathrm{WVT} = \left(\frac{G}{t}\right) A \quad [\mathrm{g\ m^2\ h^{-1}}] \quad (2)$$

where G/t is the linear slope for the change in weight of a jar (G, in grams) relative to the time period that this change occurred (t, in hours), and A is the exposed area to atmosphere (in units of m^2).

3. Result and discussion

3.1. Effect of hydrolysis on the morphology of potato peel- and cotton-derived cellulose nanocrystals

The yields of both cotton- and potato peel-CNC derived from their respective sources of extracted cellulose by acid hydrolysis were similar at 41–42% (dry cellulose basis), which appeared comparable to the quoted yield of 44% for cotton CNC in the literature (Dong et al., 1998). The synthesis method appeared equally suited to both sources of cellulose, except in the case of the potato variant a 50% longer reaction time was required to reach the same product in appearance (as well differentiated CNC particles). The hydrolysis reaction was initially limited to 60 min for the potato cellulose to match the cotton species; however, large segments of aggregated microfibrils were still observed by TEM as being present in the reacting mixture. The difference in performance using the same reaction condition may be ascribed to variant microstructures between the different species of cellulose (Hamad, 2008). As a result, the hydrolysis reaction for the potato cellulose required 90 min to complete satisfactorily.

Fig. 1 presents TEM micrographs of example products for the two species of cellulose nanocrystals, showing few remaining microfibrils with most particles appearing as isolated, rod-like fibers having nanoscale dimensions. Fig. 2 summarizes the length

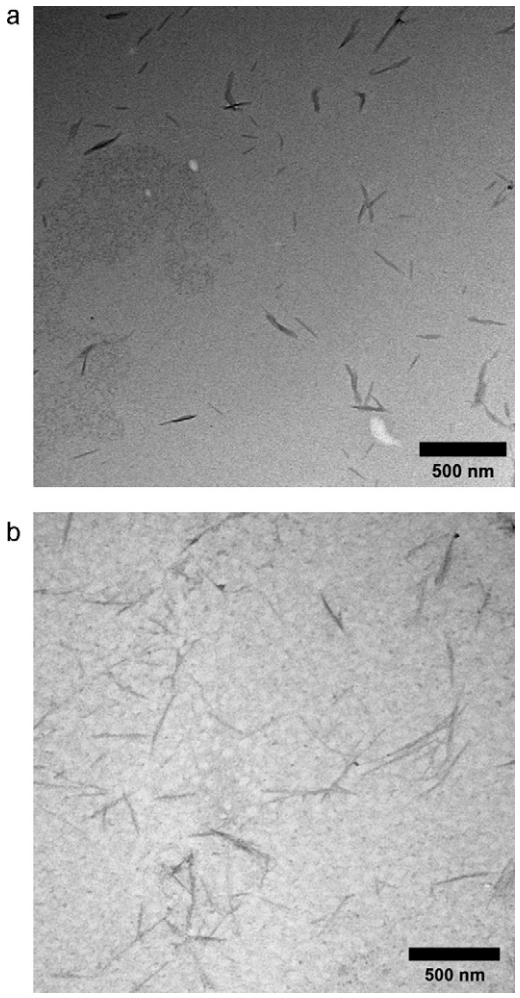

Fig. 1. TEM micrographs of cellulose nanocrystals prepared from (a) cotton and (b) potato cellulose. Scale bar represents 500 nm.

distributions estimated from the TEM images for both cotton and potato CNC. The nanocrystals from cotton displayed a relatively narrow length distribution with an average of 226 ± 65 nm (stated uncertainty being the standard deviation of the population). Comparatively, the CNC fibers from potato peel waste exhibited a much broader distribution with many longer fibers in comparison to

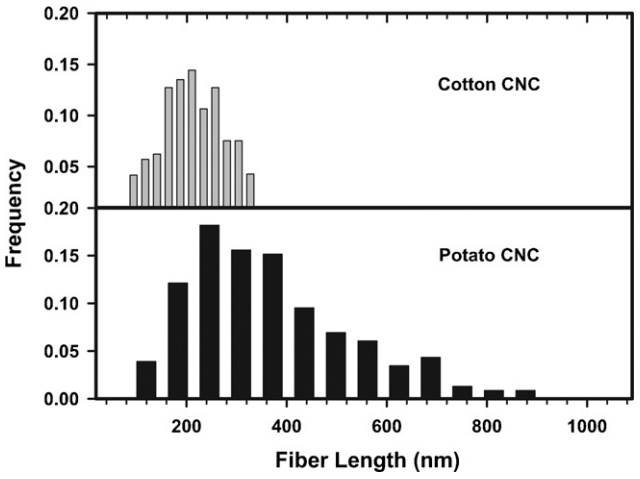

Fig. 2. Particle length distribution measured by TEM for cellulose nanocrystals prepared from cotton and potato cellulose.

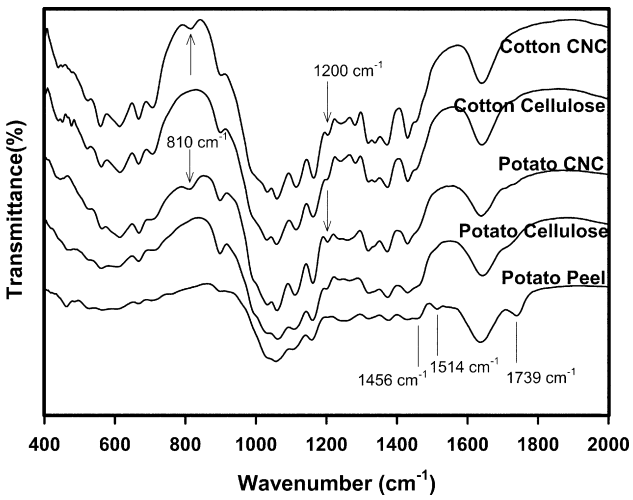

Fig. 3. Infrared spectra of untreated potato peel, extracted cellulose from potato and cotton, and their corresponding CNC prepared by acid hydrolysis.

cotton. The average length of the potato CNC was 410 ± 181 nm. The diameters of both CNC appeared comparable in the micrographs with an estimated value of 10 nm, thus giving a nominal aspect ratio of 23 for the cotton variant and aspect ratio of 41 for potato. The fiber length for the cotton CNC matched those reported in the literature (Dong et al., 1998; Miller & Donald, 2003) while no values could be found for potato peel-derived CNC. However, the lengths of the potato CNC fibers were not unusual, being similar to that of other plant-prepared CNC, such as sisal CNC (aspect ratio of 43; Siqueira, Bras, & Dufresne, 2009), wheat straw CNC (aspect ratio of 45; Helbert, Cavaillé, & Dufresne, 1996) and *Luffa Cylindrica* CNC (aspect ratio of 47; Siqueira, Bras, & Dufresne, 2010).

As a matter of interest, the hydrolysis reaction was performed with cotton cellulose for 90 min to match the conditions used with potato peel waste. The resulting CNC sample was analyzed and found to have a length of 183 ± 66 nm and aspect ratio of 18. Not unexpectedly, the hydrolysis conditions influenced the fiber dimensions (Habibi et al., 2010). If we continued to use comparable reaction conditions in this study then the cotton CNC would be foreseeably disadvantaged in the testing as a mechanical reinforcement aid by its further shortening of length. Therefore, for the remainder of this discussion only the samples corresponding to hydrolysis conditions that yielded maximum fiber length from each biosource were used.

3.2. FTIR characterization of CNC

Fig. 3 shows the mid-range infrared spectra of potato and cotton cellulose at different stages in the chemical procedure, namely untreated potato peel, extracted cellulose sources from potato peel and cotton, as well as CNC. The large bands at 3300–3500 cm^{-1} (assigned to O—H stretching) and near 2900 cm^{-1} (assigned to C—H stretching) were found for all characterized materials. Three vibrational bands were unique to only the untreated potato peel at 1739 cm^{-1}, 1514 cm^{-1} and 1456 cm^{-1}, with the former band attributed to the C=O stretching vibration of acetyl and uronic ester groups of hemicellulose as well as the ester linkage of the carboxyl group in lignin (Li et al., 2009; Sun, Xu, Sun, Fowler, & Baird, 2005) whereas the latter two bands were assigned to the C=C vibration in lignin (Rosa et al., 2010). The region of 800–1500 cm^{-1} is a unique fingerprint region for cellulose where the majority of peaks in that range were found for all samples, indicating that regardless of alkali or acid treatment the cellulose maintained a similar chemical structure to the original untreated species. The only differences seen in

Table 1
Melting properties of the PVA films.

	Neat	Potato CNC		Cotton CNC	
	0%	1%	2%	1%	2%
Melting temperature, T_m (°C)	177	177	194	180	192
Melting enthalpy (J/g)	6.65	6.54	9.62	6.23	11.83

the fingerprint region were for the two peaks at 1200 cm^{-1} and 810 cm^{-1} found only in the acid hydrolyzed cellulose, i.e. cotton CNC and potato peel CNC, which may be assigned to the half-ester sulfate groups produced by sulfuric acid hydrolysis (Lu & Hsieh, 2010).

3.3. X-ray diffraction of CNC

Fig. 4 shows the X-ray diffraction patterns of CNC derived from (a) cotton and (b) potato peel. Both samples showed three distinctive diffraction peaks at $2\theta = 14.7°$, 16.4°, and 22.6°, which were assigned to the cellulose I crystalline structure (Wada, Heux, & Sugiyama, 2004). The result corroborated the infrared analysis in confirming the crystalline structure of both CNC species were identical to their neat, untreated cellulose sources, i.e. the crystalline structure of cellulose was unaltered by acid hydrolysis in this work. The sharp diffraction peak for the (0 0 2) plane at $2\theta = 22.6°$ indicated high perfection of the crystal lattice. The crystallinity index of cotton CNCs and potato peel CNC was comparable, calculated as 91% and 85%, respectively according to the Segal equation.

3.4. Thermal properties of the prepared films

Four types of polymer–CNC composites (TPS/PCN, TPS/CCN, PVA/PCN and PVA/CCN) were prepared to study the effects of CNC attributes and matrix compatibility on several end-use properties, where PCN refers to potato peel-derived CNC and CCN refers to cotton-derived CNC. The thermal properties of these polymer films were analyzed by DSC to determine how addition of CNC altered the formed microstructure of the polymer matrices upon solvent evaporation. The TPS films exhibited no thermal transitions within the range of temperatures analyzed, confirming complete gelatinization of the starch during film preparation but finding no influence of the CNC on the polymer structure. The PVA films, despite their high transparency, showed a small, broad melting transition from approximately 165–205 °C. Table 1 summarizes the peak melting temperatures (T_m) and melting enthalpies for the different PVA films. At 1% CNC loading, the melting transition of the polymer was unaffected by the nanofiller inclusion yet at 2% CNC addition there was a small increase in T_m by ~10 °C and the melting enthalpy increased by approximately 60%. The effect was similar regardless whether the CNC was derived from potato or cotton sources. Using an enthalpy value of 156 J/g for 100% crystalline PVA (Probst, Moore, Resasco, & Grady, 2004), the estimated crystallinity in the PVA films only increased from 4% to at best 7.5% going from 0% CNC to 2% CNC which as will be observed in the mechanical testing section below, had minimal impact on properties of the films.

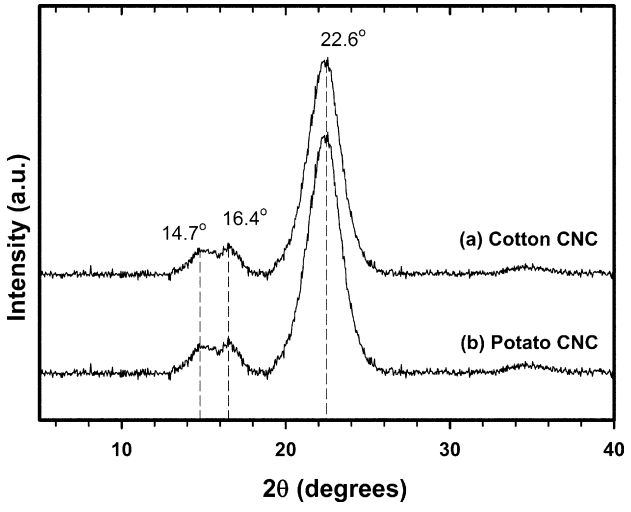

Fig. 4. X-ray diffraction patterns of CNC derived from (a) cotton and (b) potato peel.

3.5. Morphology of the prepared CNC-filled polymer films

The dispersion of CNC within the two polymer matrices was evaluated by SEM to determine whether any significantly sized aggregates formed during the casting process which would affect mechanical and water barrier properties. Typical micrographs of the films are presented in Fig. 5, which in this case correspond to films with PCN filler, showing no visible nanocrystalline cellulose aggregates in the images. None of the films with either CCN or PCN displayed any notable aggregates for either polymer matrix in the analysis by SEM. Cao et al. (2007) similarly found a uniform dispersion at CNC concentrations of 10% or lower whereas they noted white dots in SEM images for CNC aggregates at higher concentrations.

The micrographs may not have noted issues with the dispersion of the CNC in the polymer matrices, but it was evident that a few granules of starch remained intact from the procedure for preparing the TPS films. In light of the absence of crystallinity in the TPS films found by DSC analysis, it is likely these are ghost remnants of the granule where all intermolecular associations related to the original crystalline structure have been disrupted. Though few in detectable numbers, these intact granules were noted in all TPS films including those prepared without CNC. Such inhomogeneity in the matrix was a likely source of the increased uncertainty in measurements of mechanical properties, but should not have altered the relative difference between different films based on the concentration of CNC present.

3.6. Mechanical properties of the prepared films

The tensile modulus of each film was determined to evaluate improvements in the mechanical stiffness as a result of CNC incorporation; tensile strength and elongation-at-break were not included in this work due the still brittleness of the thermoplastic starch (despite inclusion of glycerol) which resulted in more defects during cutting of its tensile specimens than with PVA, making comparison based on these properties unreliable. Fig. 6(a) and (b) shows the Young's moduli of both starch and PVA films increasing with increasing PCN content. With comparable plasticizer content (30%, w/w glycerol) in both polymers, the matrix of thermoplastic starch showed a modulus that was an order of magnitude larger than PVA. With 1% PCN loading, the modulus increased by 19% and 33% for the TPS and PVA matrices, respectively. By 2% PCN, the modulus had increased by 38% and 49% for the TPS and PVA matrices, respectively. The increase in elastic stiffness was found to be significant but was smaller than hoped considering the anticipated high cost to manufacture these nanofillers. However, these results for the

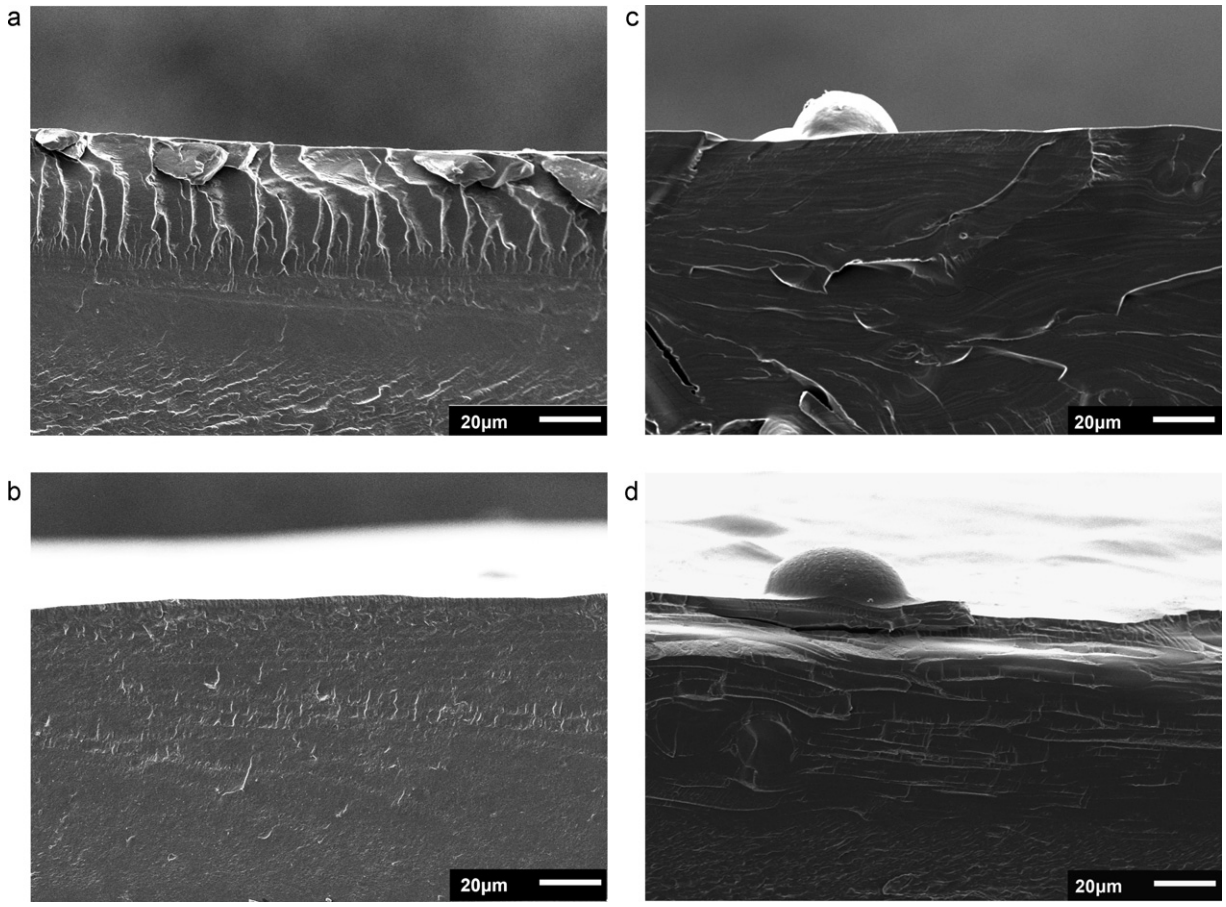

Fig. 5. SEM micrographs of potato CNC-filled polymer films, (a) 1% PCN in PVA, (b) 2% PCN in PVA, (c) 1% PCN in TPS, and (d) 2% PCN in TPS.

potato CNC were much more promise than those with cotton CNC. The addition of cotton CNC produced much smaller changes in the modulus of the PVA films (3% and 10% for 1% and 2% CCN, respectively) or TPS films (5% and 16% for 1% and 2% CCN respectively).

The lower reinforcement efficiency of either CNC in thermoplastic starch could have been due to the intact granular defects in the matrix noted by SEM; the increased noise in the analysis may have reduced the sensitivity of the analysis to the small changes made by the CNC at its low concentration. The lower reinforcement by CCN versus PCN was related to its shorter fiber length reducing its capacity to carry stresses of higher magnitude.

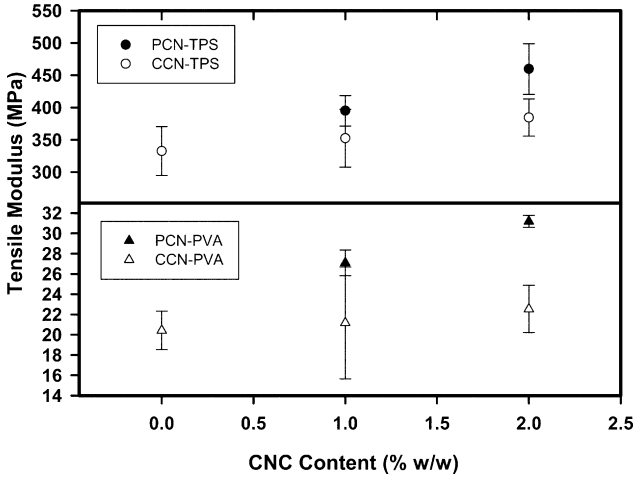

Fig. 6. Young's modulus determined by tensile testing for potato CNC (PCN)- and cotton CNC (CCN)-filled polymer films based on thermoplastic starch (TPS) or polyvinyl alcohol (PVA).

3.7. Water vapor transmission

The rate of water vapor transmission (WVT) was determined for both TPS and PVA films. The TPS films reinforced with 1% and 2% CNC (either potato or cotton) did not show a reduced WVT compared to the unfilled TPS films. This was attributed to the granule remnants creating a dominant pathway for vapor diffusion that was unaffected by the presence of the CNC though it could also be the hydrophilic properties of the TPS dominating over the small fraction of CNC being included. On the other hand, it can be seen from the plotted WVT data in Fig. 7 that the CNC-filled PVA films displayed some improvement in barrier properties compared to the neat (unfilled) PVA film, though that resistance to moisture steadily decreased over the first 60–80 h of the test. With potato CNC, the films of 1% and 2% loading were not significantly different from one another in regards to their barrier properties, though both had significantly lower WVT values for the first 60 h of testing. Films with cotton CNC may have had slightly better barrier properties compared the PCN, notably at 2% loading, but the poor reproducibility with the CCN-filled films made this uncertain. After 166 h of testing, the difference in WVT between the CNC-filled PVA films and the neat PVA film was negligible. The PCN-filled PVA films still showed a small decrease in WVT by 4% for 1% CNC loading after 166 h of testing compared to the neat film but the difference was smaller

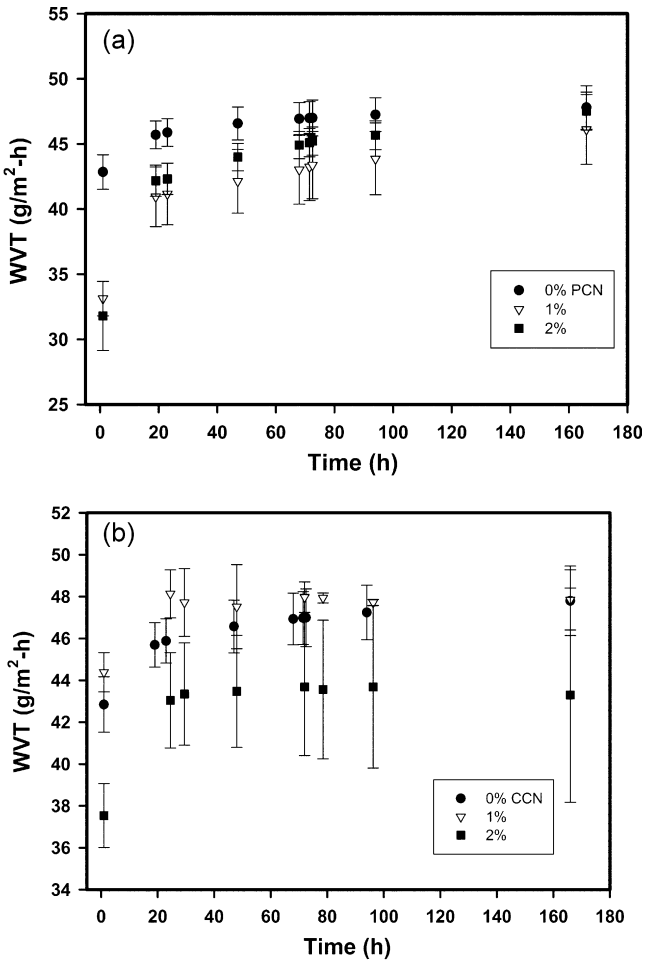

Fig. 7. Varying water vapor transmission over time for neat PVA films in comparison to films containing, (a) potato CNC (PCN) or (b) cotton CNC (CCN).

with only a 1% decrease for 2% CNC loading. The CCN-filled PVA films after 166 h showed no reduction in WVT for 1% CNC loading but did still show a 9% decrease for 2% CNC loading compared to the neat PVA film.

For the early period of testing (first 60–80 h), an improved barrier to water vapor was present due to the presence of the CNC. A uniform dispersion of CNC should force gas molecules to traverse a tortuous path to pass through the polymer film and thus act to retard gas transmission (Ramires & Dufresne, 2011). However, the improved barrier properties diminished after 80 h of testing due an increasing amount of water being absorbed over time, likely aided by the glycerol added to the polymer matrix. The hydrogen bonds between PVA/PVA and PVA/CNC species were being steadily disrupted and water gained access into further regions of the film more easily as a result. The plasticization resulting from the increased water absorption was evident by the center of the films which were drawn downwards into the test assembly as time progressed.

4. Conclusion

The results from this study have shown that cellulose nanocrystals can be derived by potato peel waste, in comparison to other notable nanocrystals reported in the literature, especially cotton CNC. Extracted cellulose from potato required 50% longer time during acid hydrolysis compared to cotton to obtain well differentiated fibers from the original microfibrils but resulted in significantly longer nanoparticle in the end product at comparable yield. Mechanical and barrier properties were improved by the incorporation of these CNC into a polymer matrix, even at low loadings of 1–2%, but only when the chemistry of the matrix was distinctly different from that of cellulose. Despite the improvements made by the inclusion of these CNCs in the tested polymer films, the changes were small when factoring in consideration of the cost to prepare them relative to other comparable commercial fillers like nanoclays or carbon nanotubes.

Acknowledgements

The authors wish to express their appreciation to the ABIP BioPotato Network (co-leaders: Drs. Helen Tai and Yvan Pelletier) under Agriculture and Agri-Food Canada as well as the Natural Science and Engineering Research Council of Canada (NSERC) for their funding of this project, as well as Manitoba Starch for their generosity in donations of the potato starch.

References

Azizi Samir, M. A. S., Alloin, F., & Dufresne, A. (2005). Review of recent research into cellulosic whiskers, their properties and their application in nanocomposite field. *Biomacromolecules*, *6*, 612–626.

Cao, X., Dong, H., & Li, C. M. (2007). New nanocomposite materials reinforced with flax cellulose nanocrystals in waterborne polyurethane. *Biomacromolecules*, *8*(3), 899–904.

Dinand, E., Chanzy, H., & Vignon, M. R. (1996). Parenchymal cell cellulose from sugar beet pulp: Preparation and properties. *Cellulose*, *3*, 183–188.

Dong, X. M., Revol, J.-F., & Gray, D. G. (1998). Effect of microcrystallite preparation conditions on the formation of colloid crystals of cellulose. *Cellulose*, *5*, 19–32.

Dufresne, A. (2010). Processing of polymer nanocomposites reinforced with polysaccharide nanocrystals. *Molecules*, *15*, 4111–4128.

Dufresne, A., Dupeyre, D., & Vignon, M. R. (2000). Cellulose microfibrils from potato tuber cells: Processing and characterization of starch–cellulose microfibril composites. *Journal of Applied Polymer Science*, *76*, 2080–2092.

Eichhorn, S. J. (2011). Cellulose nanowhiskers: Promising materials for advanced applications. *Soft Matter*, *7*, 303–315.

Habibi, Y., Lucia, L. A., & Rojas, O. J. (2010). Cellulose nanocrystals: Chemistry self-assembly and applications. *Chemical Reviews*, *110*, 3479–3500.

Hamad, W. (2008). On the development and applications of cellulosic nanofibrillar and nanocrystalline materials. *The Canadian Journal of Chemical Engineering*, *84*, 513–519.

Helbert, W., Cavaillé, J. Y., & Dufresne, A. (1996). Thermoplastic nanocomposites filled with wheat straw cellulose whiskers. Part I: Processing and mechanical behavior. *Polymer Composites*, *17*, 604–611.

Keijbets, M. J. H. (2008). Potato processing for the consumer: Developments and future challenges. *Potato Research*, *51*, 271–281.

Li, R., Fei, J., Cai, Y., Li, Y., Feng, J., & Yao, J. (2009). Cellulose whiskers extracted from mulberry: A novel biomass production. *Carbohydrate Polymers*, *76*, 94–99.

Lu, P., & Hsieh, Y. L. (2010). Preparation and properties of cellulose nanocrystals: Rods, spheres, and network. *Carbohydrate Polymers*, *82*, 329–336.

Miller, A. F., & Donald, A. M. (2003). Imaging of anisotropic cellulose suspensions using environmental scanning electron microscopy. *Biomacromolecules*, *4*, 510–517.

Ostenson, M., Jarund, H., Toriz, G., & Gatenholm, P. (2006). Determination of surface functional groups in lignocellulosic materials by chemical derivatization and ESCA analysis. *Cellulose*, *13*, 157–170.

Paralikar, S. A., Simonsen, J., & Lombardi, J. (2008). Poly(vinyl alcohol)/cellulose nanocrystal barrier membranes. *Journal of Membrane Science*, *320*, 248–258.

Pereda, M., Amica, G., Rácz, I., & Marcovich, N. E. (2011). Structure and properties of nanocomposite films based on sodium caseinate and nanocellulose fibers. *Journal of Food Engineering*, *103*, 76–83.

Probst, O., Moore, E. M., Resasco, D. E., & Grady, B. P. (2004). Nucleation of polyvinyl alcohol crystallization by single-walled carbon nanotubes. *Polymer*, *45*, 4437–4443.

Qua, E. H., Hornsby, P. R., Sharma, H. S. S., Lyons, G., & McCall, R. D. (2009). Preparation and characterization of poly(vinyl alcohol) nanocomposites made from cellulose nanofibers. *Journal of Applied Polymer Science*, *113*, 2238–2247.

Ramires, E. C., & Dufresne, A. (2011, April). A review of cellulose nanocrystals and nanocomposites. *Tappi Journal*, *10*, 9–16.

Rosa, M. F., Medeiros, E. S., Malmonge, J. A., Gregorski, K. S., Wood, D. F., Mattoso, L. H. C., et al. (2010). Cellulose nanowhiskers from coconut husk fibers: Effect of preparation conditions on their thermal and morphological behaviour. *Carbohydrate Polymers*, *81*, 83–92.

Segal, L., Creely, J. J., Martin, A. E., Jr., & Conrad, C. M. (1959). An empirical method for estimating the degree of crystallinity of native cellulose using the X-ray diffractometer. *Textile Research Journal*, *29*, 786–794.

Siqueira, G., Bras, J., & Dufresne, A. (2009). Cellulose whiskers versus microfibrils: Influence of the nature of the nanoparticle and its surface functionalization on

the thermal and mechanical properties of nanocomposites. *Biomacromolecules*, *10*(2), 425–432.

Siqueira, G., Bras, J., & Dufresne, A. (2010). Luffa cylindrical as a lignocellulosic source of fiber, microfibrillated cellulose, and cellulose nanocrystals. *BioResources*, *5*, 727–740.

Sun, X. F., Xu, F., Sun, R. C., Fowler, P., & Baird, M. S. (2005). Characteristics of degraded cellulose obtained from steam-exploded wheat straw. *Carbohydrate Research*, *340*, 97–106.

Tashiro, K., & Kobayashi, M. (1991). Theoretical evaluation of three-dimensional elastic constants of native and regenerated celluloses: Role of hydrogen bonds. *Polymer*, *32*, 1516–1526.

Tawali, M. A., Omer, H. A. A., & Gad, S. M. (2008). Partial replacing of concentrate feed mixture by potato processing waste in sheep rations. *American–Eurasian Journal of Agricultural & Environmental Sciences*, *4*, 156–164.

Wada, M., Heux, L., & Sugiyama, J. (2004). Polymorphism of cellulose I family: Reinvestigation of cellulose IVI. *Biomacromolecules*, *5*, 1385–1391.